

Ellipsoid Bounds on State Trajectories for Discrete-time Systems with Time-invariant and Time-varying Linear Fractional Uncertainties

Masako Kishida and Richard D. Braatz, *IEEE Fellow*

Abstract—Polynomial-time algorithms are proposed for computing tight ellipsoidal bounds on the state trajectories of discrete-time linear systems with time-varying or time-invariant linear fractional parameter uncertainties and ellipsoidal uncertainty in the initial state. The approach employs linear matrix inequalities to determine an initial estimate of the ellipsoid, which is improved by the subsequent application of the skewed structured singular value. Tradeoffs between computational complexity and conservatism are discussed for the three algorithms. Small conservatism for the tightest bounds is observed in numerical examples used to compare the algorithms.

I. INTRODUCTION

Identifying the potential ranges for the states in an uncertain dynamical system is important in many systems engineering problems such as safety analysis [1], satellite control [2], and attitude estimation of aerospace and underwater vehicles [3]. Motivated by various applications, many papers have considered the state outer bounding problem for time-varying [4], [5], [6] and time-invariant perturbations [7], [8], [9] (see [10] for a discussion of the greater difficulty for time-invariant perturbations). The bounding of the state vector by ellipsoid has been deeply discussed in literature for discrete-time linear dynamical systems with unknown-but-bounded uncertainties (e.g., see [11], [5] and citations therein), including for additive perturbations [4], combinations of state-space matrix and additive perturbations [5], and linear fractional perturbations [6]. The relative merits of ellipsoidal and ∞ -norm-bounded uncertainty descriptions within the context of this problem have been discussed [12].

In this paper, a new approach for computing tight ellipsoidal outer bounds is presented. The approach applies to time-invariant, time-varying, and mixed parametric uncertainties, with ellipsoidal initial state uncertainties. On contrast to the vast majority of the literature that assumes that the system dynamics depend on the perturbations in a restrictive way (e.g., affine); this paper (1) treats linear fractional perturbations (as in [6]), which includes other dependencies such as polytopic, polynomial, and rational as special cases, and (2) presents algorithms that propagate the uncertain state for multiple time instances, which can dramatically reduce conservatism for both time-invariant and time-varying perturbations.

The key idea of the proposed approach is to first employ linear matrix inequalities (LMIs) [13] to estimate the orientation and ratios of axis lengths of the ellipsoid, followed

by application of the skewed structured singular value [14] to compute two-sided bounds on the size of the ellipsoid. Numerical algorithms are proposed that employ various strategies to reduce the computational cost.

Section II presents the problem statement and some mathematical background. Section III presents a preliminary analysis needed for Section IV that proposes the numerical algorithms, which are applied and compared in numerical examples in Section V. Section VI concludes the paper.

II. PROBLEM STATEMENT AND MATHEMATICAL BACKGROUND

The problem statement is summarized below.

Problem 2.1: Let $x_k, c_k \in \mathbb{R}^n$ denote the state and nominal state vectors at time instance $k \in \{0, 1, 2, \dots\}$, $p \in \mathbb{R}^m$ denote a vector of uncertain real parameters, and $T : \mathbb{R}^n \times \mathbb{R}^m \rightarrow \mathbb{R}^n$ be a linear fractional function of its arguments. Given an uncertain value for the initial states x_0 ,

$$(x_0 - c_0)^T E_0 (x_0 - c_0) \leq 1, \quad E_0 > 0, \quad (1)$$

and discrete-time uncertain dynamical system

$$x_{k+1} = T(p)x_k, \quad p_{\min} \leq p \leq p_{\max}, \quad k = 0, 1, 2, \dots, \quad (2)$$

determine an ellipsoidal outer bound on the state vector x_k specified by $E_k > 0$, and c_k , $k = 1, 2, 3, \dots$, such that

$$\min \log \det E_k^{-1} \quad (3)$$

subject to $E_k > 0$ and $(x_k - c_k)^T E_k (x_k - c_k) \leq 1$,

$$\forall x_k \in S_k = \{x_k \text{ satisfying (1) and (2)}\}.$$

The set of linear fractional functions $\{T\}$ includes the sets of polytopic, polynomial, and rational functions (e.g., [15]). The objective (3) is to determine, for each time instance, the ellipsoid of minimum volume that outer bounds the state vector.¹ This paper proposes to approach Problem 2.1 through a combination of LMIs and the skewed structured singular value, applied to T written in terms of a linear fractional transform (LFT) of a structured perturbation matrix.

Definition 2.2 (Mixed Structured Perturbation [15]):

A mixed structured perturbation Δ is a matrix with the

M. Kishida is with University of Illinois at Urbana-Champaign and Massachusetts Institute of Technology (MIT), ksd@mit.edu

R. D. Braatz is with MIT braatz@mit.edu

¹Alternative objectives, such as minimizing the trace as in [6], can be addressed by the algorithms in this paper by slightly modifying the first step of the LMI formulation.

specified structure:

$$\Delta = \text{diag}\{\delta_1^r I_{k_1}, \dots, \delta_{m_r}^r I_{k_{m_r}}, \delta_1^c I_{k_{m_r+1}}, \dots, \delta_{m_c}^c I_{k_{m_r+m_c}}, \Delta_{m_r+m_c+1}^C, \dots, \Delta_{m_r+m_c+m_c}^C\},$$

with real scalars δ_i^r , complex scalars δ_j^c , and full complex blocks $\Delta_q^C \in \mathbb{C}^{k_{m_r+m_c+q} \times k_{m_r+m_c+q}}$. The integers m_r , m_c , m_C , and k_i define the structure of the perturbation. A real scalar δ_i^r (or complex scalar δ_i^c) is said to be *repeated* if the integer $k_i > 1$.

Definition 2.3 (Linear Fractional Transformation [15]):

A mapping $F_u : \mathbb{C}^{q_1 \times p_1} \rightarrow \mathbb{C}^{p_2 \times q_2}$ of the form

$$F_u(N, \Delta_p) = N_{22} + N_{21} \Delta_p (I - N_{11} \Delta_p)^{-1} N_{12},$$

with

$$N = \begin{bmatrix} N_{11} & N_{12} \\ N_{21} & N_{22} \end{bmatrix} \in \mathbb{C}^{(p_1+p_2) \times (q_1+q_2)}, \quad \Delta_p \in \mathbb{C}^{q_1 \times p_1},$$

such that $(I - N_{11} \Delta_p)^{-1}$ exists, is a (*upper*) *linear fractional transformation* (LFT) (see Fig. 1a).

A noninvertable $I - N_{11} \Delta_p$ occurs for some perturbation Δ_p of interest if and only if the LFT is ill-posed. The existence of the inverse of $I - N_{11} \Delta_p$ for the perturbations Δ_p under consideration can be evaluated using the structured singular value [15]. To simplify the presentation, this paper assumes that this verification is carried out before applying the algorithms.

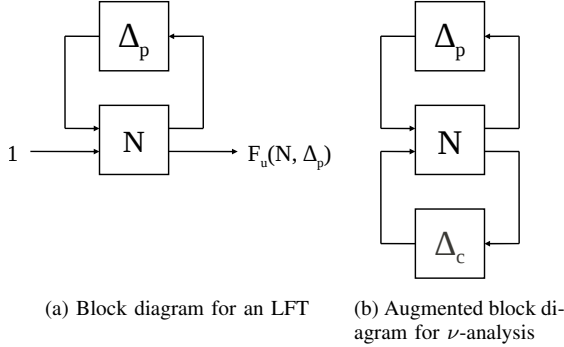


Fig. 1: LFTs and Main Loop Theorem

To express an uncertain parameter vector p defined by box constraints in terms of an LFT, define

$$p = p_c + W_p \delta \bar{p}, \quad |\delta \bar{p}_j| \leq 1, \\ p_c = \frac{1}{2}(p_{\max} + p_{\min}), \quad W_p = \frac{1}{2} \text{diag}\{p_{\max} - p_{\min}\},$$

then, the uncertain system (2) can be written as

$$x_{k+1} = T(p_c + W_p \delta \bar{p}) x_k \quad (4)$$

$$= F_u(N, \Delta_p) x_k \quad (5)$$

where

$$N = \begin{bmatrix} N_{11} & N_{12} \\ N_{21} & N_{22} \end{bmatrix}, \quad \Delta_p = \text{diag}\{\delta \bar{p}_1 I_{k_1}, \dots, \delta \bar{p}_m I_{k_p}\},$$

where the values of k_i depend on the order and structure of the map T .

The transformation from (4) to (5) is always possible for any well-posed linear fractional function by using block-

diagram algebra [15], and for any well-posed polynomial or rational function by application of multidimensional realization algorithms [16]. The LFT for any particular function is not unique, and LFTs are desired in which the dimension of Δ_p is minimal, so as to minimize the computational cost of the proposed algorithms. Multidimensional model reduction algorithms (e.g., see [17] and references cited therein) can be applied to an LFT to reduce its dimensions before applying the proposed algorithms.

The outer bounding algorithms employ the skewed structured singular value.

Definition 2.4 (Skewed Structured Singular Value [14]):

The skewed structured singular value of N with respect to $\Delta = \text{diag}\{\Delta_1, \Delta_2\}$, where Δ_1 and Δ_2 are two structured perturbations, is defined by

$$\nu_{\Delta}(N) = \begin{cases} (\min\{k | \exists \Delta = \text{diag}\{\Delta_1, k \Delta_2\} \text{ with } \|\Delta_i\| \leq 1 \\ \text{and } \det(I - N \Delta) = 0\})^{-1} \\ 0, \text{ if no } k \text{ or } \Delta \text{ exist such that } \det(I - N \Delta) = 0 \end{cases}$$

where $\|\cdot\|$ is the induced matrix 2-norm.

Upper and lower bounds on ν can be computed in polynomial time, with no more effort than non-skewed structured singular value calculations [18], [19], by a variety of methods including power iterations and linear matrix inequalities. The next result relates the LFT (5) for the uncertain system (2) to the skewed structured singular value ν .

Theorem 2.5 (Scaled Main Loop Theorem [14], [18]):

For any well-posed LFT in the uncertain dynamical system $x_{k+1} = F_u(N, \Delta_p) x_k$,

$$\max_{\|\Delta_p\| \leq 1} \|F_u(N, \Delta_p)\| = \nu_{\Delta}(N), \\ \text{where } \Delta = \begin{bmatrix} \Delta_p & 0 \\ 0 & \Delta_C \end{bmatrix}, \quad \|\Delta_C\| \leq 1,$$

and Δ_C is a complex full-block perturbation.

By defining N appropriately, this result can also be applied to compute bounds on the minimum diameter of an ellipsoid that overbounds the state vector when the ellipsoid's axis orientations and relative lengths are pre-specified. The next section gives some preliminary analysis used in the subsequent derivation of LMI-based algorithms for determining the ellipsoid's axis orientations and relative lengths.

III. PRELIMINARY ANALYSIS: UNCERTAINTY ONLY IN THE INITIAL STATE

For a known nonsingular linear system, (2) simplifies to

$$x_{k+1} = T x_k.$$

Given a state x_k with uncertainty that can take any value within the ellipsoid,

$$(x_k - c_k)^T E_k (x_k - c_k) \leq 1, \quad E_k > 0,$$

an outer bounding ellipsoid parameterized by $E_{k+1} > 0$ and c_{k+1} satisfies

$$(x_{k+1} - c_{k+1})^T E_{k+1} (x_{k+1} - c_{k+1}) \leq 1$$

for all $x_{k+1} \in S_{k+1}$. By application of the S-procedure [20], the state is outer bounded by this ellipsoid if and only if there exists $\lambda \geq 0$ that satisfies the linear matrix inequality

$$\begin{bmatrix} T^T E_{k+1} T & -T^T \hat{c}_{k+1} & 0 \\ -\hat{c}_{k+1}^T T & -1 & -\hat{c}_{k+1}^T T \\ 0 & -T^T \hat{c}_{k+1} & -T^T E_{k+1} T \end{bmatrix} - \lambda \begin{bmatrix} E_k & -E_k c_k & 0 \\ -c_k^T E_k & c_k^T E_k c_k - 1 & 0 \\ 0 & 0 & 0 \end{bmatrix} \leq 0,$$

where $\hat{c}_{k+1} = E_{k+1} c_{k+1}$ (detailed derivation not given here due to space constraints).² A solution to this LMI for invertible T that gives an ellipsoid of minimum volume is (see Section 4.3 of [21])

$$E_{k+1} = T^{-T} E_k T^{-1}, \quad c_{k+1} = T c_k,$$

which occurs for $\lambda = 1$. From the Loewner-Behrend Theorem [22], [23], this minimum-volume ellipsoid is unique.

Repeating the above procedure from the uncertain initial condition implies that the minimum-volume ellipsoids for all time instances k are given by

$$E_k = (T^{-T})^k E_0 (T^{-1})^k, \quad c_k = T^k c_0. \quad (6)$$

These ellipsoidal covers on the states are exact, which can be observed checking the map between the boundary of the ellipsoid at time instance k to the boundary of the ellipsoid of time instance $k + 1$.

Remark 3.1: The above analysis can be generalized to singular T . If T is singular, then there exist nonzero $x_1 \in S_k$ that map to the origin and x_1 and all subsequent x_k lie in a lower dimensional space. This lower dimensional space and its covering ellipsoid are of dimension $n - m$, where n is the dimension of the matrix T and m is the number of zero eigenvalues of T .

The next section addresses uncertain state matrices.

IV. PROPOSED ALGORITHM: UNCERTAIN SYSTEMS

Due to space limitations, this section describes the case of $c_k = 0$ for all k (the analysis is similar for $c_k \neq 0$). Application of the S-procedure implies that E_{k+1} specifies an outer bounding ellipsoid for x_{k+1} for fixed T if

$$T^T E_{k+1} T \leq E_k,$$

with the E_k specifying the minimum-volume ellipsoid when the inequality is an equality (6). The following algorithms employ this LMI to address uncertainties in the state matrix.

A. Algorithm I: One Step Ahead

This algorithm applies to time-varying perturbations. Recall that the uncertain system (2) is written as

$$x_{k+1} = F_u(N, \Delta_p) x_k, \quad \|\Delta_p\|_2 \leq 1,$$

$$\text{where } x_k^T E_k x_k \leq 1, \quad E_k > 0,$$

²This derivation is simpler than an equivalent LMI derived elsewhere [6].

is given. The minimum-volume ellipsoid is described by

$$\min \log \det E_{k+1}^{-1} \quad (7)$$

subject to

$$E_{k+1} > 0, \quad (8)$$

$$F_u(N, \Delta_p)^T E_{k+1} F_u(N, \Delta_p) - E_k \leq 0. \quad (9)$$

For general LFTs, it is straightforward to apply the proof technique in [24] to show that this nonconvex optimization is NP-hard. An approximate solution Y for E_{k+1} can be obtained by replacing (9) by the

- nominal system: $F_u(N, 0)^T Y F_u(N, 0) - E_k \leq 0$, or
- average: $\bar{F}_u(N, \Delta_p)^T Y \bar{F}_u(N, \Delta_p) - E_k \leq 0$, where $\bar{F}_u(N, \Delta_p)$ is an elementwise averaged matrix over multiple sampled Δ_p within the uncertainty set, or
- extreme uncertainties: $F_u(N, \Delta_{p,i})^T Y F_u(N, \Delta_{p,i}) - E_k \leq 0$, $i = 1, \dots, 2^m$, where m is the dimension of parameter p .

An improved solution to (7) can be obtained by combining one of the approximations for (9) with the application of ν to determine an optimal scaling of the ellipsoid. Remember that the approximate solution was used to fix the shape of the ellipsoid, and does not mean approximate covering of the states. For specificity, the steps are described for the case when extreme uncertainties are used, with similar steps for the other cases.

Step 1: Solve
$$\min \log \det Y_k^{-1}$$

subject to

$$Y_k > 0,$$

$$F_u(N, \Delta_{p,i})^T Y_k F_u(N, \Delta_{p,i}) - E_k \leq 0, \quad i = 1, \dots, 2^m,$$

where each $\Delta_{p,i}$ has ± 1 as its diagonal elements.

Step 2: Set

$$M_{k+1,11} = N_{11}, \quad M_{k+1,12} = N_{12},$$

$$M_{k+1,21} = Y_k^{1/2} N_{21} E_k^{-1/2}, \quad M_{k+1,22} = Y_k^{1/2} N_{22} E_k^{-1/2},$$

and compute upper and lower bounds on $\nu_\Delta(M_{k+1})$.

Step 3: The ellipsoidal bound on the state

$$\frac{1}{\nu_\Delta^2(M_{k+1})} x_{k+1}^T Y_k x_{k+1} \leq 1, \quad (10)$$

$$x_{k+1}^T E_{k+1} x_{k+1} \leq 1, \quad E_{k+1} = \frac{1}{\nu_\Delta^2(M_{k+1})} Y_k,$$

is the ellipsoid of minimum volume with rotation and relative magnitude of axes defined by Y_k . Replacing ν with its upper bound in (10) results in an ellipsoid that is guaranteed to cover the state x_{k+1} for all perturbations within the uncertainty description.

Instead of propagating the state, this algorithm propagates the ellipsoidal bound on the state at each time instance k (i.e., E_0 is used to compute E_1 , E_1 is used to compute E_2 , etc.), with approximately constant computational cost per time instance.

B. Algorithm II: Compound

This algorithm can treat each real parametric uncertainty as being time-invariant or time-varying and propagates the

state instead of the state bounds between time instances, which requires the use of a new N and Δ_p for each time instance. The only uncertainty at each time instance is in the initial state x_0 and the uncertain parameters. The structure of Δ_p in the ν computations depend on the time dependency of each uncertain parameter. At each time instance k , with the given initial uncertainty E_0 , E_k is computed using the same expressions for Algorithm I but with different N and Δ_p constructed using standard methods [15]. For the special case of all parameters being time-invariant, these N and Δ_p are constructed from $F_u(N, \Delta_p)^k$. Analytical expressions for these LFTs are available [15].

C. Algorithm III: Receding Horizon

This algorithm combines the update strategies in Algorithms I and II, so as to be more computationally efficient than Algorithm II, but with the introduction of potential conservatism. The algorithm employs a moving horizon s : at each time instance $k \leq s$, this algorithm coincides with Algorithm II. As each time instance $k > s$, E_k is computed from E_{k-s} by using $F_u(N, \Delta_p)^s$ for time-invariant parameters.

TABLE I: Comparison of Algorithms*

At k th step	I	II	III
Comp. Cost Ratio	1	k	$\min\{k, s\}$
Bounds	possibly loose	tight	moderate
Dependency	x_{k-1}	x_0	x_{k-1-s} to x_{k-1}

* Same for both time-invariant and time-varying.

V. NUMERICAL EXAMPLES

The proposed algorithms are compared in three numerical examples with upper and lower bounds on each uncertain parameter. The upper and lower bounds on ν were computed by using YALMIP [25] and the Skew Mu Toolbox (SMT) [26]. To simplify the discussion, bounds on each uncertain parameter are assumed to be time-invariant regardless of whether the uncertainty is time-invariant or time-varying.

A. Coordinate Transformation

This simple example is a discrete-time variation of a continuous-time problem used to evaluate the accuracy of state-bounding algorithms in handling rotations in the state vector [27]. These examples are useful model problems because many state-bounding algorithms applied to such systems can produce conservatism approaching ∞ as $k \rightarrow \infty$ [27].

The numerical example is a coordinate transformation that rotates and scales the state vector:

$$\begin{bmatrix} x_{1,k+1} \\ x_{2,k+1} \end{bmatrix} = \alpha \begin{bmatrix} 1 & p \\ -p & 1 \end{bmatrix} \begin{bmatrix} x_{1,k} \\ x_{2,k} \end{bmatrix},$$

where $x_{1,k}$ and $x_{2,k}$ are the states at time instance k , p is a parameter, and α is a scaling constant. The choice $\alpha = 1/\sqrt{1+p^2}$ describes state vectors that rotate in 2 dimensions. Bounds on each state are computed from LFTs derived for each state at each time instance k .

The associated LFTs are summarized below, to clearly delineate the differences between the three algorithms. The

systems can be written in terms of LFTs as

$$\begin{aligned} \begin{bmatrix} x_{1,k+1} \\ x_{2,k+1} \end{bmatrix} &= F_u(N, \Delta_p) \begin{bmatrix} x_{1,k} \\ x_{2,k} \end{bmatrix}, \quad (\text{Alg. I}) \\ &= F_u(N_k, \Delta_{p,k}) \begin{bmatrix} x_{1,0} \\ x_{2,0} \end{bmatrix}, \quad (\text{Alg. II}) \\ &= F_u(N_s, \Delta_{p,s}) \begin{bmatrix} x_{1,s-k} \\ x_{2,s-k} \end{bmatrix}, \quad (\text{Alg. III}) \end{aligned}$$

$$\text{where } N = \begin{bmatrix} 0_2 & I_2 \\ \alpha \begin{bmatrix} 0 & w_p \\ -w_p & 0 \end{bmatrix} & \alpha \begin{bmatrix} 1 & p_c \\ -p_c & 1 \end{bmatrix} \end{bmatrix}, \quad (11)$$

$$\Delta_p = \delta \bar{p} I_2,$$

and N_k , N_s , $\Delta_{p,k}$ and $\Delta_{p,s}$ are given by the expressions for multiplication of LFTs [15]. The time dependency of the parameters appears in the structures of $\Delta_{p,k}$ and $\Delta_{p,s}$.

The ellipsoidal outer bounds for Algorithms I-III for uncertain parameter p are indistinguishable from the exact outer bounding ellipsoid for $p \in [0.9, 1.1]$ and $\alpha = 1/\sqrt{2}$ (see Fig. 3). The outer bounding ellipsoids produced by Algorithms I-III are different for $p \in [-0.3, 0.3]$ and $\alpha = 1$, with Algorithm II with time-invariant p having the smallest conservatism and Algorithm I with time-varying p having the largest, as expected from the theoretical derivations in Section V (see Fig. 4). None of the algorithms have the large conservatism reported by some other methods [27]. Algorithm I, which treats the parameter as being time-varying, ranged from producing the same tight outer ellipsoids as Algorithms II-III to producing larger ellipsoids (compare Figs. 3 and 4).

B. Quasi-Coordinate Transformation

Consider the system

$$\begin{bmatrix} x_{1,k+1} \\ x_{2,k+1} \end{bmatrix} = \alpha \begin{bmatrix} 1 & p+q \\ p-q & 1 \end{bmatrix} \begin{bmatrix} x_{1,k} \\ x_{2,k} \end{bmatrix},$$

where p is an uncertain parameter of unknown sign and q is a known parameter. For $q^2 - p^2 > 0$ this system is obtained by discretization of a continuous-time system with uniform circular motion at constant speed with angular velocity $\omega = \sqrt{q^2 - p^2}$ and unit mass and radius, x_1 is the x -coordinate for a point on a unit circle, and x_2 is an intermediate state that relates the x -coordinate to the acceleration and position of the point ($d^2 x_1 / dt^2 = -\omega^2 x_1$). For $q = 0$, this system is a positive gradient system (negative spring constant) where the potential function is proportional to its position x_1 with proportionality constant p^2 , and x_2 is an intermediate state. Mechanisms with negative spring constants appear in mechanical design [28] and in the context of post-buckled structures and objects [29], [30].

By defining

$$q = p_c, \quad p = w_p \delta p,$$

$$N = \begin{bmatrix} 0_2 & I_2 \\ \alpha \begin{bmatrix} 0 & w_p \\ w_p & 0 \end{bmatrix} & \alpha \begin{bmatrix} 1 & p_c \\ -p_c & 1 \end{bmatrix} \end{bmatrix}, \quad \Delta_p = \delta \bar{p} I_2. \quad (12)$$

The only difference between (11) and (12) is the sign of an element in N_{21} . LFTs for Algorithm II and III can be constructed in a similar manner as in Example A.

This system has much more interesting dynamic propagation of the uncertain state (see Figs. 5-7), especially for $q = 0$ and a large range for p where the set of possible states is highly nonconvex with four spokes (see Fig. 7). Algorithm II produced very tight outer bounds on the state trajectories for both time-invariant and time-varying uncertainty (see Figs. 5) and 6).

C. Mass/Spring System

The system of two linear springs and a unit mass in Fig. 2 has an overall spring constant of

$$k = \frac{1}{\frac{1}{k_1} + \frac{1}{k_2}} = \frac{k_1 k_2}{k_1 + k_2}. \quad (13)$$

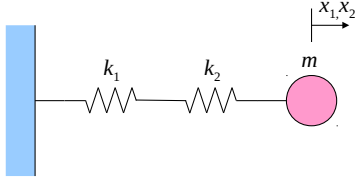


Fig. 2: Mass/Spring System

Let x_1 be the position of the mass from its rest position, x_2 be the velocity of the mass, and h be the time step. The equation of motion of the system is

$$\begin{aligned} \begin{bmatrix} x_{1,k+1} \\ x_{2,k+1} \end{bmatrix} &= \left(\begin{bmatrix} 1 & 0 \\ 0 & 1 \end{bmatrix} + h \begin{bmatrix} 0 & 1 \\ -k & 0 \end{bmatrix} \right) \begin{bmatrix} x_{1,k} \\ x_{2,k} \end{bmatrix} \\ &= F_u(N, \Delta_p) \begin{bmatrix} x_{1,k} \\ x_{2,k} \end{bmatrix}, \quad (\text{Alg. I}) \end{aligned}$$

where

$$\begin{aligned} N &= \begin{bmatrix} N_{11} & N_{12} \\ N_{21} & N_{22} \end{bmatrix}, \quad \Delta_p = \text{diag}\{\delta \bar{k}_1 I_2, \delta \bar{k}_2 I_2\}, \\ N_{11} &= \begin{bmatrix} \frac{w_1}{k_{1,c} + k_{2,c}} & w_1 & -\frac{w_2}{k_{1,c} + k_{2,c}} & w_2 k_{1,c} \\ 0 & 0 & 0 & w_2 \\ -\frac{w_1}{k_{1,c} + k_{2,c}} & w_1 & -\frac{w_2}{k_{1,c} + k_{2,c}} & w_2 k_{1,c} \\ 0 & 0 & 0 & 0 \end{bmatrix}, \\ N_{12} &= \begin{bmatrix} k_{1,c} k_{2,c} & 0 \\ k_{2,c} & 0 \\ k_{1,c} k_{2,c} & 0 \\ 1 & 0 \end{bmatrix}, \quad N_{21} = \begin{bmatrix} 0 & h w_1 / (k_{1,c} + k_{2,c})^2 \\ 0 & -h w_1 / (k_{1,c} + k_{2,c}) \\ 0 & h w_2 / (k_{1,c} + k_{2,c})^2 \\ 0 & -h k_{1,c} w_2 / (k_{1,c} + k_{2,c}) \end{bmatrix}^T, \\ N_{22} &= \begin{bmatrix} 1 & h \\ \frac{k_{1,c} k_{2,c} h}{k_{1,c} + k_{2,c}} & 1 \end{bmatrix}. \end{aligned}$$

LFTs for Algorithm II and III can be constructed in a similar manner as in Example A. All three algorithms produced tight outer ellipsoids on the state for time-invariant uncertainty in the two spring constants, with the ellipsoids from Algorithm II being especially tight (see Fig. 8).

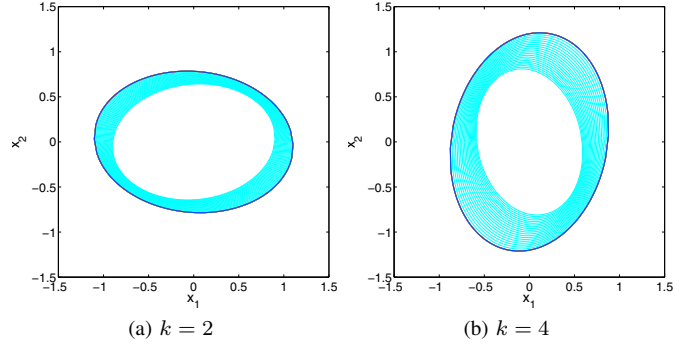


Fig. 3: Outer ellipsoids for Ex. A with uncertain parameter $p \in [0.9, 1.1]$ and $\alpha = 1/\sqrt{2}$. The ellipsoids for time-invariant and time-varying p are indistinguishable for this example. In all figures in this paper: the curves are the boundaries of the ellipsoids, Alg. I is red (ν upper bound) and orange (ν lower), Alg. II is purple (ν upper) and magenta (ν lower), Alg. III is green (ν upper) and blue (ν lower), and gridded fixed values for p within the uncertainty set are cyan. All examples used ellipsoidal uncertain initial set centered at $(0, 0)$ with $E_0 = [2 \ 0; 0 \ 1]$, $s = 3$, and Step 1 with extreme points in the solution of the LMI optimization.

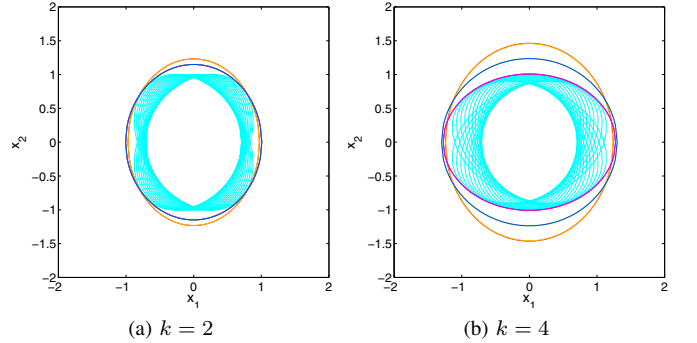


Fig. 4: Outer ellipsoids for Ex. A with time-invariant $p \in [-0.3, 0.3]$ and $\alpha = 1$.

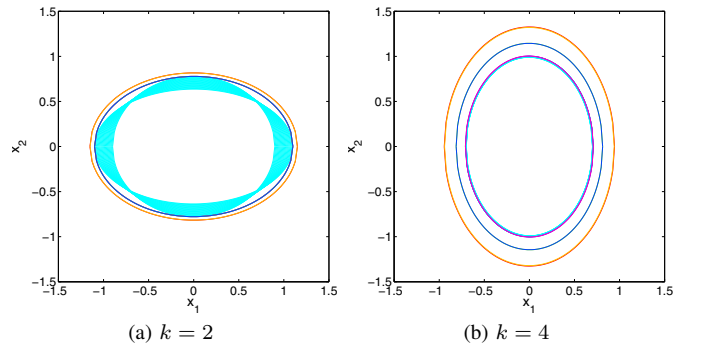


Fig. 5: Outer ellipsoids for Ex. B with $p \in [-0.1, 0.1]$, $q = 1$, and $\alpha = 1/\sqrt{2}$ for Alg. I and time-invariant p in Alg. II and III and the sample state trajectories.

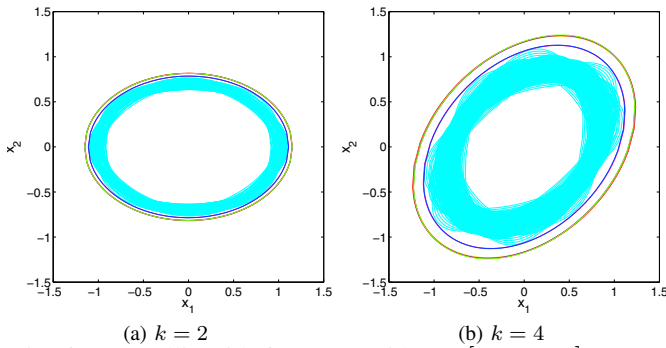


Fig. 6: Outer ellipsoids for Ex. B with $p \in [-0.1, 0.1]$, $q = 1$, and $\alpha = 1/\sqrt{2}$, with time-varying p in all algorithms and sample state trajectories.

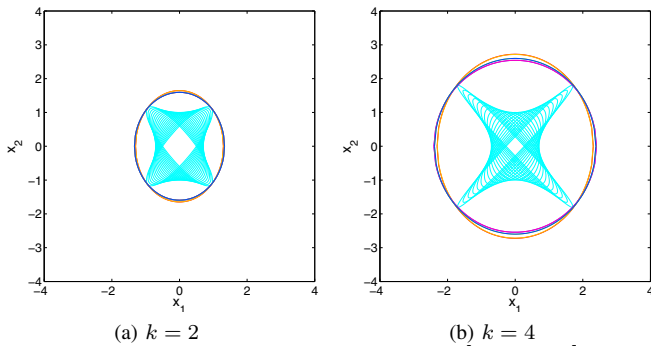


Fig. 7: Outer ellipsoids for Ex. B with $p \in [-0.3, 0.3]$, $q = 0$ and $\alpha = 1$ for Alg. I and time-invariant p in Alg. II and III and the sample state trajectories.

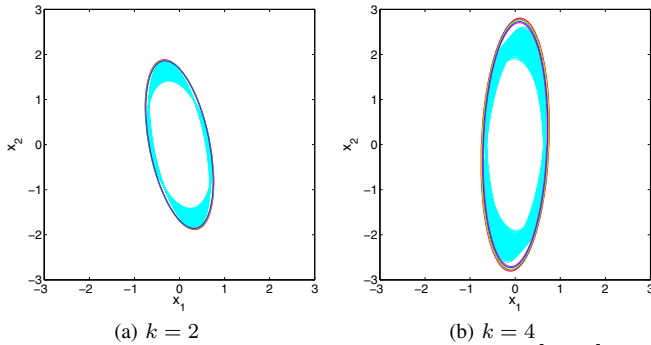


Fig. 8: Outer ellipsoids for Ex. C with $k_1 \in [8, 12]$ and $k_2 \in [8, 12]$ and $h = 0.2$ for Alg. I and time-invariant p in Alg. II and III and the sample state trajectories.

VI. CONCLUSIONS

Algorithms are presented for computing ellipsoidal bounds on the state trajectories of discrete-time linear systems with ellipsoidal uncertainty on the initial state and time-varying or time-invariant real parametric uncertainties. Upper and lower bounds on the minimum size of the ellipsoid were determined by using the skewed μ , with rotation and ratios of the axis lengths determined by solving quasi-convex LMI-based optimizations. The algorithms apply to systems with linear fractional dependence on the model parameters, which includes the polynomial and rational dependencies that commonly occur in applications.

Alg. I has the lowest computational cost, but can be conservative if applied to a system with time-invariant uncertainties, or if the actual reachable sets of states are not ellipsoids. Alg. II produced tight bounds for polynomial systems with either time-varying or time-invariant parameter uncertainties but is computationally expensive. Alg. III employs a moving horizon to reduce the computational cost of Alg. II, while increasing conservatism. The moving horizon can be specified in Alg. III to trade off computational cost with tightness of the bounds, and this algorithm is the most practical for computing outer ellipsoids for large k for systems with time-invariant uncertainties.

VII. ACKNOWLEDGMENTS

The authors acknowledge support from the Institute for Advanced Computing Applications and Technologies.

REFERENCES

- [1] H. Huang, C. Adjiman, and N. Shah, *AIChE J.*, 48:78–96, 2002.
- [2] D. Y. Rokityanski and S. M. Veres, *Math. & Comp. Mod. of Dyn. Sys.*, 11:239–249, 2005.
- [3] A. K. Sanyal, T. Lee, M. Leok, and N. H. McClamroch, *Sys. & Cont. Letters*, 57:236–245, 2008.
- [4] C. Durieu, E. Walter, and B. Polyak, *JOTA*, 111:273–303, 2001.
- [5] B. T. Polyak, S. A. Nazin, C. Durieu, and E. Walter, *Automatica*, 40:1171–1179, 2004.
- [6] L. El Ghaoui and G. Calafiore, “Worst-case simulation of uncertain systems,” in *Robustness in Identification and Control*. Springer, 1999.
- [7] D. T. Horak, *AIAA JGCD*, 11:508–516, 1988.
- [8] B. Tibken and E. P. Hofer, *Appl. Math. Comp.*, 70:329–338, 1995.
- [9] M. Kishida, P. Rumschinski, R. Findeisen, and R. D. Braatz, “Efficient polynomial-time outer bounds on state trajectories for uncertain polynomial systems using skewed structured singular values,” in *Proc. of the IEEE MSC*, 2011, in press.
- [10] V. Puig, A. Stancu, and J. Quevedo, “Simulation of uncertain dynamic systems described by interval models: A survey,” in *Proc. of the 16th IFAC World Congress*, Prague, 2005, paper Fr-A13-TO/6.
- [11] F. C. Schweppe, *IEEE TAC*, 13:22–28, 1968.
- [12] F. L. Chernousko, “Optimal ellipsoidal estimates of uncertain systems: An overview and new results,” in *Coping with Uncertainty*. Springer, 2010.
- [13] S. Boyd, L. E. Ghaoui, E. Feron, and V. Balakrishnan, *Linear Matrix Inequalities in System and Control Theory*. SIAM, 1994.
- [14] R. S. R. Smith, Ph.D. dissertation, Caltech, Pasadena, CA, 1990.
- [15] K. Zhou, J. C. Doyle, and K. Glover, *Robust and Optimal Control*. Prentice Hall, 1995.
- [16] E. L. Russell, C. P. H. Power, and R. D. Braatz, *Int. J. of Robust & Nonlinear Control*, 7:113–125, 1997.
- [17] E. L. Russell and R. D. Braatz, *Comput. Chem. Eng.*, 22:913–926, 1998.
- [18] M. K. H. Fan and A. Tits, *Sys. & Cont. Letters*, 18:409–421, 1992.
- [19] G. Ferreres, *A Practical Approach to Robustness Analysis with Aeronautical Applications*. Springer, 1999.
- [20] S. Boyd and L. Vandenberghe, *Convex Optimization*. Cambridge University Press, 2004.
- [21] F. C. Schweppe, *Uncertain Dynamic Systems*. Prentice-Hall, 1973.
- [22] M. Berger, *Géométrie*. Paris: CEDIC/Nathan, 1979.
- [23] L. Pronzato and E. Walter, *Automatica*, 30:1731–1739, 1994.
- [24] R. D. Braatz, P. M. Young, J. C. Doyle, and M. Morari, *IEEE TAC*, 39:1000–1002, 1994.
- [25] J. Löfberg, “YALMIP: A toolbox for modeling and optimization in MATLAB,” in *Proc. of the CACSD Conference*, Taipei, Taiwan, 2004, pp. 284–289.
- [26] G. Ferreres and J. M. Biannic, *Skew Mu Toolbox (SMT)*, 2009.
- [27] R. Moore, *Interval Analysis*. Prentice-Hall, 1996.
- [28] R. Pelrine, R. Kornbluh, J. Joseph, R. Heydt, Q. Pei, and S. Chiba, *Mat. Sci. & Eng.: C*, 11:89–100, 2000.
- [29] Y. C. Wang and R. S. Lakes, *J. of Composite Materials*, 39:1645–1657, 2005.
- [30] Z. P. Bazant and L. Cedolin, *Stability of Structures: Elastic, Inelastic, Fracture, and Damage Theories*. Oxford University Press, 1991.